Mind blanking is associated with a rigid spatio-temporal profile in typical wakefulness

Sepehr Mortaheb[1,2], Manousos A. Klados[3], Laurens Van Calster[4,5], Paradeisios Alexandros Boulakis[1], Kleio Georgoula[1], Steve Majerus[2,4,5], and Athena Demertzi[1,2,4,5*]

[1]Physiology of Cognition Lab, GIGA-Consciousness, University of Liège, Liège, Belgium

[2]Fund for Scientific Research FNRS, Brussels, Belgium

[3]Department of Psychology, CITY College, University of York Europe Campus, Thessaloniki, Greece

[4]Psychology and Neuroscience of Cognition Research Unit, University of Liège, Liège, Belgium

[5]GIGA-Cyclotron Research Center In Vivo Imaging, University of Liège, Liège, Belgium

[*]Corresponding Author: Athena Demertzi

Email: a.demertzi@uliege.be

Address: Physiology of Cognition Lab, GIGA-Consciousness, GIGA Research Institute B43, Avenue de l'Hôpital 11, 4000 Liège, Belgium

Abstract

Mind-blanking (MB) is the inability to report mental contents, challenging the view of a constantly thought-oriented mind during wakefulness. Using fMRI experience-sampling we show that MB is reported scarcely, fast, and has low transitional dynamics, pointing to its role as a transient mental relay. MB's cerebral profile is linked to an overall positive connectivity pattern, bearing great resemblance to neural configurations observed in local sleeps, possibly reflecting neuronal silencing during wakefulness. We also find less efficient information flow between the default mode (DMN) and other networks before reporting MB. The DMN-salience network segregation was further able to classify MB from other reports in fewer steps, suggestive of an early saliency evaluation of contentless phenomenology along the neurocognitive hierarchy. Collectively, MB's unique neurofunctional profile among thought-oriented reports supports the view of instantaneous mental absences happening during wakefuless, paving the way for more mechanistic investigations of this particular phenomenology during ongoing mentation.

1 Introduction

During spontaneous thinking we tend to traverse different mental states which recruit the activity of multiple neural systems[1]. What is interesting is that, apart from entertaining specific thoughts, there are moments when our minds go nowhere, giving the impression that we are empty of mental content. These phenomenological occurrences are known as content-free awareness[2] or mind blanking (MB)[3]. What is the position of MB among other mental states during ongoing thinking, and how does the brain configure to support this empty-mind phenomenology?

Behavioral studies indicate that MB happens scarcely during everyday functioning, yet with a considerable frequency. It has been shown, for example, that during focused tasks, MB was reported on average 14.5% of the time whenever subjects were requested to provide a mental evaluation[3], and 18% of the time when participants reported MB by self-catching[4]. MB was also observed in the form of attentional lapses, when participants were engaged in task performance[5–7]. In terms of neural underpinnings, there was evidence for reduced fMRI functional connectivity between the default mode network (DMN) and frontal, visual, and salience networks when participants were instructed to "think of nothing" as compared to "let your mind wander"[8]. MB was also associated with deactivation of Broca's area and parts of the hippocampus, as well as with activation of the anterior cingulate cortex, which was interpreted as reduced inner speech[9]. Decreased functional connectivity in the posterior regions of the DMN and increased connectivity in the dorsal attentional network were also found in an experienced meditator practicing content-minimized awareness[2]. Collectively, these studies indicate that the investigation of MB is rising over the years. Yet, MB so far has been induced, therefore the estimation of its occurrences across time can be biased. Also, MB has been examined in highly-trained individuals, like experienced meditators, therefore limiting the generalizability of its occurrences in typical participants. Finally, the neural substrates associated with MB concern a limited number of brain regions, leaving the whole-brain functional connectome uncharted.

The importance of a comprehensive characterization of MB rests on the fact that MB challenges the view of a primarily thought-oriented mind, which traverses stimulus-dependent and stimulus-independent thoughts[10]. Mind states which are thought-oriented indeed prevail during wakeful mentation and are characterized by rich spatio-temporal dynamics at the brain level[11]. Inversely, less complex neural architectures of highly segregated organization and less metastable dynamics are linked to the inability to report subjective experience as seen in sleep[12], anesthetized primates[13], typical individuals under anesthesia[14], and in vegetative/unresponsive patients[15]. Several theoretical models concur that the reason we cannot report in such a segregated state is because the brain is unable to combine divergent signals and distribute them widely so that they become reportable[16,17]. These theoretical frameworks further hold that the inability to report mental contents can also happen in a brain state with extreme functional integration. In this scenario, an abnormally large number of regions work in synchrony, and, as a result, the brain becomes no longer capable of processing information in a way that leads to reportability, such as during generalized epilepsy[18] and local sleeps[19]. As both neural configurations can occur during ongoing mentation[15] and can be linked to the inability to report, the emerging question is which one would support the phenomenology of MB. To date, no empirical evidence favours one possibility over the other.

With the aim to delineate the neurofunctional profile of MB, we used fMRI-based experience-sampling in typical individuals[20] in order to: a) account for a representative behavioral quantification of pure (no induction) MB occurrences in a dynamic way, b) determine MB's functional connectome at the whole-brain level, and c) estimate the brain's segregative/integrative organization whenever reporting MB occurrences.

Results

Data were acquired from 36 typical participants (27 females, 9 males, mean age: 23y±2.9) within a 3T MRI scanner. Randomly presented auditory sounds (n=50) prompted subjects to evaluate and report their mental content as it was prior the probe. Possible mental states were: i) MB, ii) perception of sensory stimuli without internal thoughts (Sens), iii) stimulus-dependent thoughts (SDep), and iv) stimulus-independent thoughts (SInd). With this setup, Rest periods and Response-type periods could be determined (Fig.1A).

Behavioral reports

We found that MB was reported significantly fewer times than any other mental state (median=2.5, IQR=3, min=0, max=9; Fig.2A). There was a main effect of mental state with respect to reaction times ($\chi^2(3) = 66.63$, $p < 0.001$; generalized linear mixed model analysis with gamma distribution and inverse link function), with MB being reported faster than SDep ($z = 3.81$, $p = 0.0008$) and SInd ($z = 3.37$, $p = 0.0042$) but with no differences from Sens ($z = -0.73$, $p = 0.89$; post-hoc Tukey test; Fig.2B). The evaluation of the dynamic transitions among different mental states showed exceptionally low, but equal probabilities (0.06) of reporting MB departing from a content-oriented state. Inversely, departures from MB towards content-oriented reports were characterized by high transition probabilities (>0.27). Also, the probability to re-enter MB (i.e. reporting another MB immediately after a MB report) was particularly low (0.04, Fig.2C). Finally, the hypothesis for a uniform distribution of reports across the session could not be rejected either for MB ($\chi^2(9) = 12.31$, $p = 0.20$, $\phi = 0.35$; Fig.2D) or for SDep ($\chi^2(9) = 5.25$, $p = 0.81$, $\phi = 0.10$) and SInd ($\chi^2(9) = 4.22$, $p = 0.90$, $\phi = 0.07$). However, Sens reports were not equally distributed over time ($\chi^2(9) = 18.15$, $p = 0.03$, $\phi = 0.23$).

Brain patterns and neurofunctional analysis

By means of phase-based coherence connectivity analysis and k-means clustering, we determined four brain patterns which appeared recurrently across the rest periods (Fig.1B). The patterns were characterized by distinct signal configurations: a pattern of complex inter-areal interactions, containing positive and negative phase coherence values between long-range and short-range regions (Pattern 1), a pattern showing signal anti-correlations primarily between the visual network and the other networks (Pattern 2), a pattern with overall positive inter-areal phase coherence (Pattern 3), and a pattern of overall low inter-areal coherence (Pattern 4, Fig.3A). In terms of occurrences, Pattern 4 appeared at a significantly higher rate than Pattern 1 ($t(35) = 6.23$, $p < 0.001$, Cohen's $d = 1.04$), Pattern 2 ($t(35) = 5.27$, $p < 0.001$, Cohen's $d = 0.88$) and Pattern 3 ($t(35) = 5.50$, $p < 0.001$, Cohen's $d = 0.92$, p-values are FDR corrected at $\alpha = 0.05$; Fig.3B).

To determine which brain pattern was the closest to MB reports, we used the cosine distance as the similarity measure between five connectivity matrices preceding a report (i.e., Response-type periods) and the four brain patterns (Fig. 1C). Using a generalized linear mixed model fit to the distance measures of each brain pattern separately, we found a significant effect of mental state for distance values to Pattern 3 ($\chi^2(3) = 15.47$, $p = 0.001$) and Pattern 4 ($\chi^2(3) = 8.83$, $p = 0.032$). Pattern 3 further showed higher similarity to MB compared to the reports about Sens ($Estimate = 0.09$, $z = 2.71$, $p = 0.034$), SDep ($Estimate = 0.11$, $z = 3.48$, $p = 0.003$), and SInd thoughts ($Estimate = 0.12$, $z = 3.82$, $p < 0.001$; Post-hoc tukey tests, Fig.4).

Information flow analysis

To determine each mental state's integration/segregation profile, we used diffusion maps followed by mental state classification. Diffusion-map analysis is a non-linear dimensionality reduction technique based on spectral graph theory[21]. Applied to brain data, a larger distance in the diffusion values between regions indicates smaller between-region transition probabilities, which implies that information exchange is less efficient. For each mental state report, diffusion maps were calculated on the average of response-type connectivity matrices related to that state. We found that for MB, diffusion values have larger distances between regions of the DMN (red range values) and what is broadly defined as the salient network (blue range values). Furthermore, the diffusion value distance was smaller for content-oriented reports (Fig.5A). Using subjects' maps as feature vectors and applying a C4.5 decision tree classifier with a 10-fold cross validation scheme, mental state classification was achieved at an accuracy of 81.16% (Table1 and Table2). Based on the classifier's optimum decision tree and the brain regions' diffusion values, the somatomotor network was the region whose diffusion value separated MB from thought-oriented reports (Fig.5B). Subsequently, the final classification between thought-oriented reports (SDep vs. SInd) was achieved with the contribution of DMN prefrontal regions. Similarly, MB classification was achieved when the diffusion value was <0.6 in the left fronto-insular cortex (salience network). When the diffusion value in this region was higher, the decision between MB and Sens reports required more steps and the contribution of right parietal areas, bilateral visual, and left temporal cortices (Fig.5B).

Discussion

We investigated the neurofunctional profile of mind blanking (MB) and found that it occupies a unique position among though-oriented reports during spontaneous mentation. By means of experience-sampling within the fMRI environment, we first show that typical individuals have few number of MB reports, which are reported faster than other mental states. These findings are in line with previous studies showing that MB gets reported significantly less often than thought-related content[20]. Our results are also in line with studies reporting similarly fast MB reaction times while participants are involved in sustained attention to response task[7,22]. Nevertheless, in other investigations MB is reported more slowly compared to other mental states, which is interpreted as MB facilitating sluggishness in responses[23] or as the result of decreases in alertness and arousal during task performance[5]. Here, we consider that the fast reaction times for MB and the longer reaction times for thought-oriented reports (SDep, SInd) might be attributed to an additional cognitive evaluation of the latter. In other words, when thoughts are occupied by content, they are translated in longer cognitive evaluation as to the particularities of their content. In that respect, MB, being defined as content-free state, is reported faster. This interpretation supports previous investigations using self-paced focused reading with self-catches of MB and mind wandering, which tested how these mental modes affect reading comprehension[3].

Regardless of this heterogeneity, it can be generally concluded that MB gets reported despite its content-less phenomenology. Therefore, MB can be considered as one more mental state which contributes to spontaneous mentation. Its role among the content-oriented states is here determined by the performed dynamic analysis. We show that the probabilities in reporting MB (after reporting another state) are low, but equal. At the same time, departures from MB are more likely to lead toward content-oriented thoughts, and less likely to lead towards MB again. Collectively, these results indicate that MB might not be driven by any specific mental content, therefore serving as a transient mental relay[24]. In other words, thoughts with content can lead towards more mental contents due to semantic associations, hence creating the perception of a stream of consciousness. Since MB is not semantically associated with any particular mental content, it does not occur frequently during spontaneous thinking. As such, phenomenologically content-less reports might have less of an anchoring effect than content-full reports. The eventual finding of a uniform distribution of MB reports over time, also reported elsewhere[3,25], further suggests that MB is not a result of fatigue, and therefore confirms its unique place as a default mental state during spontaneous mentation.

By investigating whole-brain time-varying functional connectivity during the resting periods of the experience-sampling task, we show four distinct brain patterns occurring across time. These brain patterns bear great resemblance with what we previously reported as recurrent brain configurations during pure resting state fMRI acquisitions across healthy individuals and brain-injured patients[15]. The fact that these patterns appear across independent datasets, and that they are present also in non-human primates[26], utilizing different paradigms and different brain parcellations, points to their universality and robustness. Our finding that Pattern 4 (low inter-areal connectivity) shows the highest occurence probability in comparison to the other patterns, is exlpained by the fact that this configuration has the highest similarity to the underlying structural connectome[15]. As such, this pattern may act as a foundation upon which the others can occur, by showing divergence of function from structure, which is linked to mental flexibility[27]. On the other hand, an all-to-all positive inter-areal connectivity has the lowest occurrence probability and high similarity to the connectivity matrices preceding MB reports. This global inter-region positive connectivity has been previously reported to occur with high prevalence in NREM slow-wave sleep[28,29]. In this sleep stage, the brain's slow wave activity reflects minimal neuronal firing. Studies in rats[19] show that periods of neuronal silencing can happen also during wakefulness in the form of neuronal firing rate reduction leading to slow wave activity, which was indicative of local sleeps. When applied to humans, it has been argued that these instances of local sleeps can be the phenomenological counterpart of MB[23]. In that respect, wakefulness is not a physiological state of constantly on-periods of neuronal function. Rather, the fact that our brains show instances of neural down-states even during wakefulness possibly for homeostatic reasons[30], can be neurally translated as global positive connectivity and phenomenologically interpreted as MB.

This possibility is further accounted by prominent theoretical models of conscious experience. The Global Neuronal Workspace Theory (GNWT)[31] posits that a stimulus becomes reportable when some of its locally processed information becomes available to a wide range of brain regions, forming a balanced distributed network[32]. Therefore, the brain in a state of all-to-all positive connectivity provides not some, but all of its locally processed information globally so that, for a moment, no information is in a privileged state of processing and available to attention and awareness. This can also be similarly explained in the context of the supervisory attentional system (SAS)[25], whose all "action systems" (i.e. processing structures associated with particular tasks) will have the same dominance, leaving the SAS unable to choose which one to bring into awareness. This lack of differentiation is also portrayed in the Integrated Information Theory (IIT[16]). According to this theory, to generate an experience a physical system must be able to discriminate among a large repertoire of states (i.e., information). This must be done as a single system that cannot be decomposed into a collection of causally independent parts (i.e., integration). The all-to-all positive connectivity pattern is characterized by the highest level of integration and efficiency and the lowest level of segregation and modularity compared to the other brain patterns[15]. Therefore, it is implied that such a neural configuration is unable to produce high values of integrated information, leading to limited experience. Here, information flow was approximated by the diffusion-map analysis. Before MB reports, we observed a large range of diffusion values between DMN and other areas, which is indicative of low between-node transition probabilities. Therefore, MB is linked to rigid and inefficient information exchange. Such inefficient information flow between the DMN and other networks has also been reported while participants were instructed to think of nothing[8]. Finally, with respect to the left fronto-insular area (part of the salience network), we found that this region predicted MB reports when it was highly segregated from the DMN early and in few steps during the classification scheme. The involvement of the salience network does not come as a surprise. Indeed, this system has been shown to play an important role in switching between the DMN and the central executive network (CEN), making salient and important stimuli available to the focus of attention[33]. Also recently, it is shown that prestimulus activity of anterior insula predicts the conscious perception of visual stimuli, so that this region might act as a gate for conscious access[34]. In a similar line, as MB is free of phenomenological content, it can be that its saliency evaluation happens effortlessly and early on during the neurocognitive hierarchy translated in a more laxed inter-network engagement.

Our study is limited in several ways. First, the experience-sampling task utilized a probe-catching methodology. This means that participants were interrupted during spontaneous thinking by a probe, asking them to choose an appropriate report option to describe their thought-state. Such a probe-framing technique can restrict the estimation of potential phenomenological switches happening between the probes. Indeed, as the probes were appearing in pre-determined time points we cannot exclude the possibility of mental contents happening during the inter-probe intervals, and hence they were missed to be reported. Also, probe-framing can be suboptimal in capturing spontaneous thinking because it might lead to an inflated number of MB reports. This is because participants could choose this category since it was pre-established, which they could otherwise not report if they were to identify spontaneously[35]. The fact, though, that MB occurrences were not reported with a comparable high frequency to the content-oriented states might indicate that MB was evaluated in a representative way across the evaluation, leading to infrequent occurrences across participants. This small number of MB reports, in turn, could be considered problematic in terms of statistical inference. To address this issue, the analysis referred to data which were concatenated across subjects. This technique on the one hand increased the number of MB reports in our statistical models. On the other hand, this solution might have influenced the between-subject variability, which was here mitigated by assuming subjects as random effects variable in the mixed effect analysis. Finally, the high TR during the fMRI acquisition (2.04s) could also echo the temporal implications of the MB profiling. By means of simultaneous EEG-fMRI recordings, more light is expected to be shed on fine-grained temporal dynamics of MB. Such simultaneous multi-modal recordings are expected to also illuminate the assumption of slow-wave activity as the corresponding neural mechanism of MB. In the absence of vigilance monitoring with EEG or pupil diameter, this hypothesis remains to be further tested.

In conclusion, our study suggests that MB can be considered as a default mental state occupying a unique position among content-oriented thoughts. Its rigid neurofunctional profile could account for the inability to report mental content due to the brain's inability to configure complex inter-areal dynamics. The DMN-salience network segregation which appears to lead towards MB reporting, paves the way to more mechanistic explorations of MB. Collectively, MB's unique neurofunctional profile among thought-oriented reports supports the view that instantaneous mental absences can happen during wakefulness, setting this mental state at a prominent phenomenological position during ongoing mentation.

Methods

Participants

Participants were healthy right-handed dults who were French speaking, university students or graduates with at least a high school diploma without psychiatric or neurological disorders. All subjects gave their written informed consent to take part in the experiment and ethics committee of the University Hospital of Liège approved the study.

Experience-sampling task

Setup and procedure

Participants were lying restfully in the scanner with eyes open. At random times, they were interrupted by an auditory tone, probing them to report their immediate mental state via button presses. The sampling probes were randomly distributed between 30 and 60 seconds. Each probe started with the appearance of an exclamation mark lasting for 1000 ms inviting the participants to review and characterize the cognitive event(s) they just experienced. Several screens were presented in succession so participants could communicate their mental state type. The first screen offered four categories for a broad characterization of the cognitive experience: Absence, Perception, Stimulus-dependent thought, and Stimulus-independent thought. Absence was defined as mind blanking or empty state of mind. Perceptions represented the acknowledgment of a stimulus through one or more senses without any internal thought. Thoughts were distinguished as stimulus-dependent (i.e. with awareness of the immediate environment), or stimulus-independent (i.e. with no awareness of the immediate environment). For reporting, participants used two response boxes, one in each hand. Participants used an egocentric mental projection of their fingers onto the screen so that each finger corresponded to a specific mental category. Depending on the probes' trigger times and reaction times, the duration of the recording session was variable (48-58 min) across subjects. To minimize misclassification rates, participants had a training session outside of the scanner at least 24 hours before the actual session.

Behavioral statistical analysis

Analyses were performed using locally developed codes in Python and R. Six paired t-tests were used to analyze the occurrence number of each mental state (p-values were FDR-corrected with a significance level of $\alpha = 0.05$). A generalized linear mixed model with a gamma distribution and inverse link function tested the relationship between reaction times and mental states. Mental state reports were considered as fixed effects and participants were considered as the random effects with sex and age as confound variables. In case of significant main effects, post-hoc Tukey pairwise comparisons were applied. To model dynamic relationship between mind states, a Markov model was used to calculate the transition probabilities between participants' reports over the experiment. The uniformity of the distribution of each report over the acquisition duration was tested using the χ^2 test on the report times across all participants. The acquisition duration of each subject was divided into 10 equal time bins and number of reports at each bin was counted. To calculate the effect size of the χ^2 test, ϕ measure was used ($\phi = \sqrt{\frac{\chi^2}{n}}$, where n is the number of observations).

Neuroimaging

MRI acquisition

Experiments were carried out on a 3-T head-only scanner (Magnetom Allegra, Siemens Medical Solutions, Erlangen, Germany) operated with the standard transmit–receive quadrature head coil. fMRI data were acquired using a T2*-weighted gradient-echo EPI sequence with the following parameters: repetition time (TR) = 2040 msec, echo time (TE) = 30 msec, field of view (FOV) = 192 $\times$ 192 mm^2, 64 $\times$ 64 matrix, 34 axial slices with 3 mm thickness and 25% interslice gap to cover most of the brain. The three initial volumes were discarded to avoid T1 saturation effects. Field maps were generated from a double echo gradient-recalled sequence (TR = 517 msec, TE = 4.92 and 7.38 msec, FOV = 230 $\times$ 230 mm^2, 64 $\times$ 64 matrix, 34 transverse slices with 3 mm thickness and 25% gap, flip angle = 90°, bandwidth = 260 Hz/pixel) and used to correct echo-planar images for geometric distortion because of field inhomogeneities. A high-resolution T1-weighted MP-RAGE image was acquired for anatomical reference (TR = 1960 msec, TE = 4.4 msec, inversion time = 1100 msec, FOV = 230 $\times$ 173 mm, matrix size = 256 $\times$ 192 $\times$ 176, voxel size = 0.9 $\times$ 0.9 $\times$ 0.9 mm). The participant's head was restrained using a vacuum cushion to minimize head movement. Stimuli were displayed on a screen positioned at the rear of the scanner, which the participant could comfortably see using a head coil mounted mirror.

Preprocessing

Preprocessing and denoising were performed using a locally developed, freely available online, pipeline written in Python (nipype package[36]) encompassing toolboxes from Statistical Parametric Mapping 12[37], FSL 6.0[38], AFNI[39], and ART (`http://web.mit.edu/swg/software.htm`; `https://gitlab.uliege.be/S.Mortaheb/mind_blanking/`). All the functional volumes were realigned to the first volume and then, in a second pass, to their average. Estimated motion parameters were then used for artifact detection using ART toolbox. An image was defined as an outlier or artifact image if the head displacement in the x, y, or z direction was greater than 3 mm from the previous frame, if the rotational displacement was greater than 0.05 rad from the previous frame, or if the global mean intensity in the image was greater than 3 SDs from the mean image intensity for the entire scans. After skull-stripping of structural data (using FSL BET[40] with fractional intensity of 0.3), realigned functional images were registered to the bias-corrected structural image in the subject space (rigid-body transformation with normalized mutual information cost function). After extracting white matter (WM), grey matter (GM), and cerebrospinal fluid (CSF) masks, all the data and masks were transformed into the standard stereotaxic Montreal Neurological Institute (MNI) space (MNI152 with 2 mm resolution). WM and CSF masks were further eroded by one voxel. For noise reduction, we modeled the influence of noise as a voxel specific linear combination of multiple empirically estimated noise sources by deriving the first five principal components from WM and CSF masked functional data separately. These nuisance regressors together with detected outlier volumes, motion parameters and their first-order derivative were used to create a design matrix in the first-level general linear model (GLM). After smoothing the functional data using a Gaussian kernel of 6-mm full width at half-maximum, the designed GLM was fitted to the data. Before applying GLM, functional data were demeaned and detrended and all the motion-related and tissue-based regressors were first normalized and then demeaned and detrended using the approach explained in[41]. A temporal bandpass filter of 0.008 to 0.09 Hz was then applied on the residuals of the model to extract low frequency fluctuations of the BOLD signal. Schaefer atlas[42] with 100 ROIs were then used to parcellate each individual brain. Average of voxel time series in each region was considered as the extracted ROI time series and were used for further analysis.

Functional connectivity matrices

We used the phase-based coherence to extract between-region connectivity patterns at each time point of the scanning sessions[15]. For each subject i, after z-normalization of time series at each region r (i.e. $x_{i,r}(t)$), the instantaneous phase of each time series were calculated using Hilbert transform. However, in order to have a more accurate estimate of the instantaneous phase, a narrower bandpass filter was applied on the time series (Second order Butterworth filter in range [0.01-0.04] Hz), and then the Hilbert transform was applied on the time series as:

$$\hat{x}_{i,r}(t) = \frac{1}{\pi t} * x_{i,r}(t), \tag{1}$$

in which $*$ indicates a convolution operator. Using this transformation, an analytical signal was produced for each regional time series as:

$$X^a_{i,r}(t) = x_{i,r}(t) + i\hat{x}_{i,r}(t). \tag{2}$$

From this analytical signal, the instantaneous phase of each time series can be estimated as:

$$\phi_{i,r}(t) = \angle X^a_{i,r}(t) = tan^{-1}(\frac{\hat{x}_{i,r}(t)}{x_{i,r}(t)}). \tag{3}$$

After wrapping each instantaneous phase signal of $\phi_{i,r}(t)$ to the $[-\pi,\pi]$ interval and naming the obtained signal as $\theta_{i,r}(t)$, a connectivity measure for each pair of regions was calculated as the cosine of their phase difference. For example, the connectivity measure between regions r and s in subject i was defined as:

$$conn_{i,r,s}(t) \triangleq cos(\theta_{i,r}(t) - \theta_{i,s}(t)). \tag{4}$$

By this definition, completely synchronized time series lead to have a connectivity value of 1, completely desynchronized time series produce a connectivity value of zero, and anti-correlated time series produce a connectivity measure of -1. Using this approach, a connectivity matrix of 100×100 was created at each time point t of each subject i that we called it $C_i(t)$:

$$C_i(t) \triangleq [conn_{i,r,s}(t)]_{r,s}. \tag{5}$$

After collecting connectivity matrices of all time points of all participants, k-means clustering was applied on the matrices just related to the resting parts of the experiment. With this technique, four robust and reproducible patterns were extracted as the centroids of the clusters and each resting connectivity matrix was assigned to one of the extracted patterns. The occurrence rate of each pattern was simply calculated by counting the number of matrices which were assigned to each specific pattern at each subject separately. Significant differences between patterns occurrence rates were analyzed using paired t-test and FDR correction of p-values over six possible pairwise comparisons.

Neurofunctional analysis

To evaluate the similarity between mental states' functional connectivity patterns and the four main resting state recurrent functional configurations, we extracted the five connectivity matrices preceding each probe (as the functional repertoire of each specific mental state) and then calculated their cosine distance to the four main resting state patterns. Cosine distance between two sample matrices of A and B can be calculated as:

$$dist(A,B) = \frac{Tr(A^T B)}{\sqrt{Tr(A^T A) Tr(B^T B)}}, \tag{6}$$

where $Tr(.)$ indicates trace of a matrix. Subsequently, for each mental state the distribution of distances to all four centroids were created. A generalized linear mixed effect model with gamma distribution and log link function was applied to test the relationship between the distances to each pattern and the mental states. In this model, mental state reports were considered as fixed effects and participants as random effects with sex and age as confound variables.

Diffusion maps

Diffusion-map analysis is a non-linear dimensionality reduction technique based on spectral graph theory[21] that checks the information flow between nodes based on the transition probabilities denoted by the connection weight between the nodes. The resulting diffusion map summarizes that the larger the distance in the diffusion values between regions, the smaller the transition probability, which indicates less efficient information exchange.

To extract diffusion map of a sample connectivity matrix, the following steps were taken:

- For connectivity matrix $W_{100\times100}$, set all the negative weights to zero.
- Define a diagonal matrix (node strenght) $D_{100\times100}$, such that $D_{ii} = \sum_{j=1}^{100} W_{ij}$
- Create the transition probability matrix $M_{100\times100}$, such that $M_{ij} = W_{ij}/D_{ii}$ (an asymmetric matrix denoting transition probability from region i to region j)
- Create a symmetric matrix M_s with the same eigenvalues as M: $M_s = D^{1/2}MD^{-1/2}$
- Perform eigen decomposition on M_s to obtain its eigenvalues and corresponding orthonormal eigenvectors and sort them from the largest eigenvalue to the smallest.
- Take the first eigenvector as the main diffusion map of the connectivity matrix.

In this study, diffusion maps were estimated for the averaged connectivity matrices of each mental state. For the subsequent analysis, all the diffusion maps should also be aligned over the participants. Here, diffusion maps estimation and their alignment over participants have been performed using an open source package (`https://github.com/satra/mapalign`)[43]. As in this package, a singular value decomposition (SVD) technique is used to align the estimated diffusion maps, and SVD result is slightly different in various system configurations, we here report that in this study, diffusion map analysis were performed in a MacBook Pro 2018 TOUCH BAR MV962, processor Intel Core i5-8269U, using Python version 3.7.4 and Numpy version 1.17.2.

Mental state classification

Estimated diffusion maps were used as feature vectors and a C4.5 decision tree classifier[44] was used to classify mental states based on diffusion maps. This is a very efficient algorithm for representation of rule classification which locates the most robust features for the initial separation of the dataset, and then selects potential subtrees affected by noisy features, and prunes them. The pruned features are removed from the initial dataset and C4.5 re-runs since there is an improvement on the classification accuracy. In this study, the J48 (a Java implementation of C4.5 Classifier) decision tree, implemented in the Waikato Environment for Knowledge Analysis (WEKA)[45] was employed. The confidence factor (C) was set to 0.25 and the minimum number of instances per leaf (M) was set to 3. Classification accuracy was computed using the 10-fold cross validation strategy. According to this strategy, the dataset is divided into ten non-overlapping subsets (folds), where nine are used for training and one for testing. Accuracy is then defined as the ratio of the correctly classified instances divided by the total number of instances. To minimize the sampling bias, this procedure is repeated 10 times so each subset serves as a testing set and the model's overall accuracy is defined as the average of the 10 single-fold accuracies.

Acknowledgements

This work was supported by Belgian Fund for Scientific Research (FNRS). S.Mortaheb is a Research Fellow, A.Demertzi is a Research Associate, and S.Majerus is a Research Director at the FNRS. We also thank Mr Larry D. Fort for proof reading and editing the manuscript.

Author contributions statement

S.Mortaheb and A.D. conducted the research and wrote the manuscript. S.Mortaheb performed behavioral and neurofunctional data analysis. M.A.K. performed information flow analysis. P.A.B., K.G., and S.Mortaheb performed article review. L.V.C. and S.Majerus acquired the experience-sampling dataset. All authors reviewed the manuscript.

Additional information

Accession codes: All the codes used to generate results in this manuscript are accessible online via: https://gitlab.uliege .be/S.Mortaheb/mind_blanking. The dataset used in the analysis is freely accessible via the OSF page of the project: https://osf.io/gwrtc/

Competing interests: The authors declare no competing interests.

References

1. Smallwood, J. *et al.* The neural correlates of ongoing conscious thought. *Iscience* 102132 (2021).
2. Winter, U. *et al.* Content-free awareness: Eeg-fcmri correlates of consciousness as such in an expert meditator. *Front. Psychol.* **10** (2019).
3. Ward, A. F. & Wegner, D. M. Mind-blanking: When the mind goes away. *Front. psychology* **4**, 650 (2013).
4. Schooler, J. W. Zoning out while reading: Evidence for dissociations between experience and metaconsciousness jonathan w. schooler, erik d. reichle, and david v. halpern. *Think. seeing: Vis. metacognition adults children* **203** (2004).
5. Unsworth, N. & Robison, M. K. Pupillary correlates of lapses of sustained attention. *Cogn. Affect. & Behav. Neurosci.* **16**, 601–615 (2016).
6. Van den Driessche, C. *et al.* Attentional lapses in attention-deficit/hyperactivity disorder: Blank rather than wandering thoughts. *Psychol. science* **28**, 1375–1386 (2017).
7. Stawarczyk, D., François, C., Wertz, J. & D'Argembeau, A. Drowsiness or mind-wandering? fluctuations in ocular parameters during attentional lapses. *Biol. Psychol.* **156**, 107950 (2020).
8. Kawagoe, T., Onoda, K. & Yamaguchi, S. Different pre-scanning instructions induce distinct psychological and resting brain states during functional magnetic resonance imaging. *Eur. J. Neurosci.* **47**, 77–82 (2018).
9. Kawagoe, T., Onoda, K. & Yamaguchi, S. The neural correlates of "mind blanking": When the mind goes away. *Hum. brain mapping* **40**, 4934–4940 (2019).
10. Christoff, K., Irving, Z. C., Fox, K. C., Spreng, R. N. & Andrews-Hanna, J. R. Mind-wandering as spontaneous thought: A dynamic framework (2016).
11. Alavash, M., Thiel, C. M. & Gießing, C. Dynamic coupling of complex brain networks and dual-task behavior. *NeuroImage* **129**, 233–246 (2016).
12. Jobst, B. M. *et al.* Increased stability and breakdown of brain effective connectivity during slow-wave sleep: mechanistic insights from whole-brain computational modelling. *Sci. Reports* **7**, 1–16 (2017).
13. Barttfeld, P. *et al.* Signature of consciousness in the dynamics of resting-state brain activity. *Proc. Natl. Acad. Sci.* **112**, 887–892 (2014). arXiv:1408.1149.
14. Luppi, A. I. *et al.* Consciousness-specific dynamic interactions of brain integration and functional diversity. *Nat. Commun.* **10**, 1–12 (2019).
15. Demertzi, A. *et al.* Human consciousness is supported by dynamic complex patterns of brain signal coordination. *Sci. advances* **5**, eaat7603 (2019).
16. Tononi, G. Consciousness as integrated information: A provisional manifesto. *Biol. Bull.* **215**, 216–242 (2008).

17. Dehaene, S., Sergent, C. & Changeux, J.-P. A neuronal network model linking subjective reports and objective physiological data during conscious perception. *Proc. Natl. Acad. Sci.* **100**, 8520–5 (2003).

18. Blumenfeld, H. Impaired consciousness in epilepsy. *The Lancet Neurol.* **11**, 814–826 (2012). NIHMS150003.

19. Vyazovskiy, V. V. *et al.* Local sleep in awake rats. *Nature* **472**, 443–447 (2011).

20. Van Calster, L., D'Argembeau, A., Salmon, E., Peters, F. & Majerus, S. Fluctuations of attentional networks and default mode network during the resting state reflect variations in cognitive states: evidence from a novel resting-state experience sampling method. *J. Cogn. Neurosci.* **29**, 95–113 (2017).

21. Coifman, R. R. *et al.* Geometric diffusions as a tool for harmonic analysis and structure definition of data: Diffusion maps. *Proc. national academy sciences* **102**, 7426–7431 (2005).

22. Stawarczyk, D. & D'Argembeau, A. Conjoint influence of mind-wandering and sleepiness on task performance. *J. experimental psychology: human perception performance* **42**, 1587 (2016).

23. Andrillon, T., Burns, A., MacKay, T., Windt, J. & Tsuchiya, N. Wandering minds, sleepy brains: lapses of attention and local sleep in wakefulness. *bioRxiv* (2020).

24. Fornito, A., Harrison, B. J., Zalesky, A. & Simons, J. S. Competitive and cooperative dynamics of large-scale brain functional networks supporting recollection. *Proc. Natl. Acad. Sci.* **109**, 12788–93 (2012).

25. Watts, F. N., MacLeod, A. K. & Morris, L. Associations between phenomenal and objective aspects of concentration problems in depressed patients. *Br. J. Psychol.* **79**, 241–250 (1988).

26. Barttfeld, P. *et al.* Signature of consciousness in the dynamics of resting-state brain activity. *Proc. Natl. Acad. Sci.* **112**, 887–892 (2015).

27. Medaglia, J. D. *et al.* Functional alignment with anatomical networks is associated with cognitive flexibility. *Nat. Hum. Behav.* **2**, 156–164 (2018). 1611.08751.

28. Aedo-Jury, F., Schwalm, M., Hamzehpour, L. & Stroh, A. Brain states govern the spatio-temporal dynamics of resting-state functional connectivity. *Elife* **9**, e53186 (2020).

29. El-Baba, M. *et al.* Functional connectivity dynamics slow with descent from wakefulness to sleep. *PloS one* **14**, e0224669 (2019).

30. Bridi, M. C. *et al.* Daily oscillation of the excitation-inhibition balance in visual cortical circuits. *Neuron* **105**, 621–629.e4 (2020).

31. Dehaene, S., Changeux, J.-P., Naccache, L., Sackur, J. & Sergent, C. Conscious, preconscious, and subliminal processing: a testable taxonomy. *Trends Cogn. Sci.* **10**, 204–211 (2006).

32. Sergent, C. & Dehaene, S. Neural processes underlying conscious perception: experimental findings and a global neuronal workspace framework. *J. Physiol.* **98**, 374–384 (2004).

33. Menon, V. & Uddin, L. Q. Saliency, switching, attention and control: a network model of insula function. *Brain structure function* **214**, 655–667 (2010).

34. Huang, Z. *et al.* Anterior insula regulates brain network transitions that gate conscious access. *Cell Reports* **35**, 109081 (2021).

35. Weinstein, Y., De Lima, H. J. & van der Zee, T. Are you mind-wandering, or is your mind on task? The effect of probe framing on mind-wandering reports. *Psychon. Bull. Rev.* **25**, 754–760 (2018).

36. Gorgolewski, K. *et al.* Nipype: a flexible, lightweight and extensible neuroimaging data processing framework in python. *Front. neuroinformatics* **5**, 13 (2011).

37. Penny, W. D., Friston, K. J., Ashburner, J. T., Kiebel, S. J. & Nichols, T. E. *Statistical parametric mapping: the analysis of functional brain images* (Elsevier, 2011).

38. Jenkinson, M., Beckmann, C. F., Behrens, T. E., Woolrich, M. W. & Smith, S. M. Fsl. *Neuroimage* **62**, 782–790 (2012).

39. Cox, R. W. Afni: software for analysis and visualization of functional magnetic resonance neuroimages. *Comput. Biomed. research* **29**, 162–173 (1996).

40. Smith, S. M. Fast robust automated brain extraction. *Hum. brain mapping* **17**, 143–155 (2002).

41. Power, J. D. *et al.* Methods to detect, characterize, and remove motion artifact in resting state fmri. *Neuroimage* **84**, 320–341 (2014).

42. Schaefer, A. *et al.* Local-global parcellation of the human cerebral cortex from intrinsic functional connectivity mri. *Cereb. cortex* **28**, 3095–3114 (2018).

43. Langs, G., Golland, P. & Ghosh, S. S. Predicting activation across individuals with resting-state functional connectivity based multi-atlas label fusion. In *International Conference on Medical Image Computing and Computer-Assisted Intervention*, 313–320 (Springer, 2015).

44. Quinlan, J. R. C4. 5: Programs for machine learning. san francisco, ca, usa, 1993.

45. Frank, E., Hall, M. A. & Witten, I. H. *The WEKA workbench* (Morgan Kaufmann, 2016).

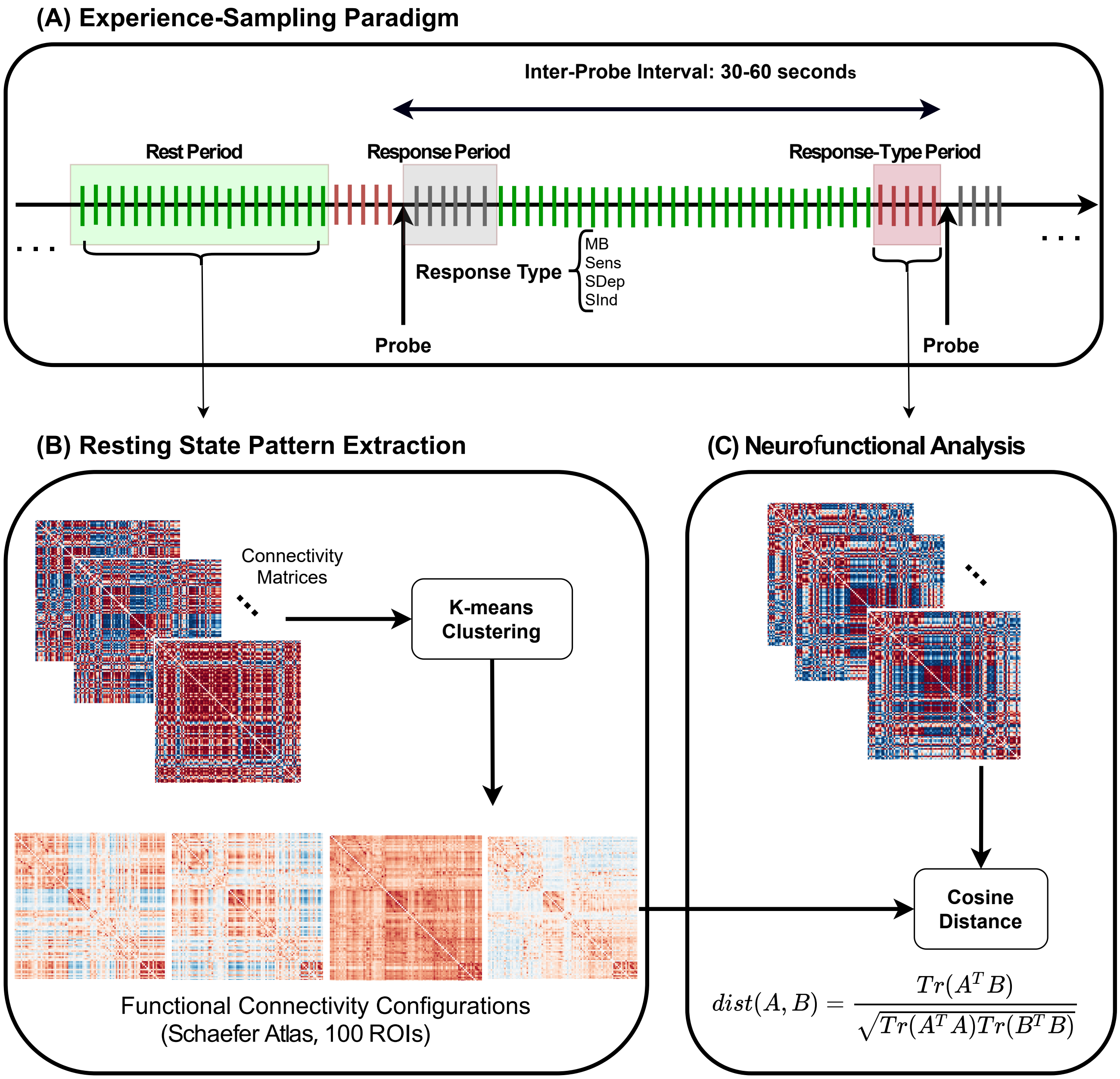

Figure 1. Experience-sampling task and analysis pipeline. (A) Participants' resting state was interrupted by auditory probes, inviting them to evaluate and report their mental state as this was before the probe, choosing among four pre-defined options (Response-types). **(B)** For brain pattern extraction, phase-based coherence was first used to estimate scan-wise connectivity matrices during the Rest Periods of the paradigm (green-shaded scans). Then, unsupervised machine learning with k-means estimated variant emerging signal configurations, which could recurrently appear across the acquisition. **(C)** To determine which brain pattern supported the reported mental states, a similarity measure was used, which compared the cosine distance between the five connectivity matrices preceding each report (red-shaded scans, Response-type periods) and the previously emerged brain patterns.

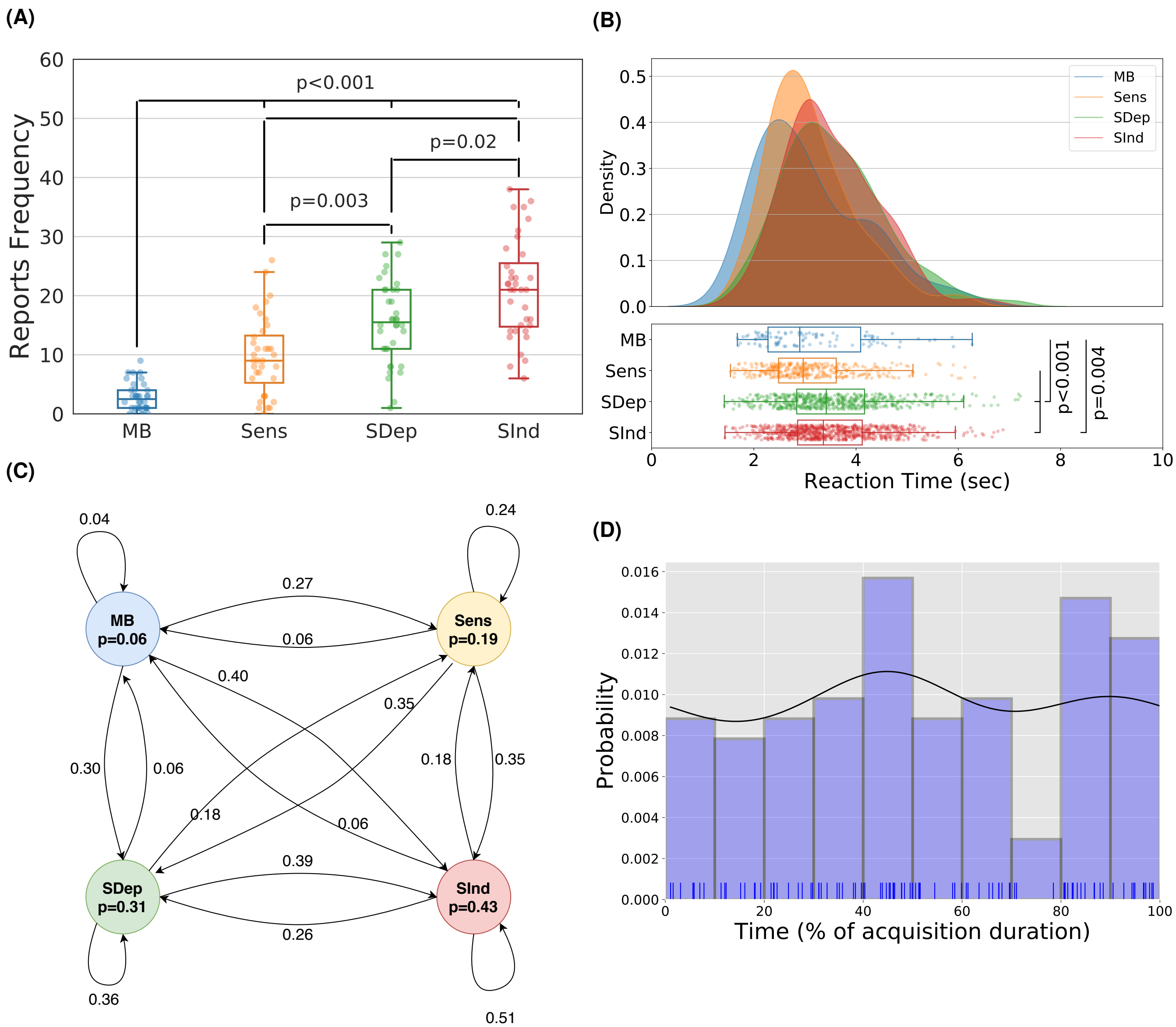

Figure 2. Mind blanking occupies a unique position among content-oriented reports. **(A)** Participants reported significantly fewer MB events than sensory-oriented (Sens), stimulus-dependent (SDep) and stimulus-independent (SInd) thoughts, confirming the less frequent yet non-negligible occurrence of MB across time (paired t-tests, FDR corrected at $\alpha = 0.05$). **(B)** Thought-oriented reports (SDep, SInd) had longer reaction times than MB and sensory-related reports, potentially due to a second-level cognitive evaluation of mental content that stimulus-related thoughts necessitated before reporting (generalized linear mixed effect model, adjusted p-values at p<0.05). **(C)** The probability of reporting MB was low yet equal when departing from content-oriented states (markov chain modelling; numbers indicate transition probability matrix values). Also, the particularly low likelihood to re-enter MB indicates that MB might not be driven by specific mental content, hence serving as a transient mental relay.**(D)** The distribution of MB reports follows a uniform shape, indicating that MB occurrences spread equally over time and therefore may comprise a default mental state. Notes: catplots represent count, boxplots represent medians with interquartile range (25th-75th percentile), histogram with 10 bins related to the equal divisions of experiment duration to its 10% time slots.

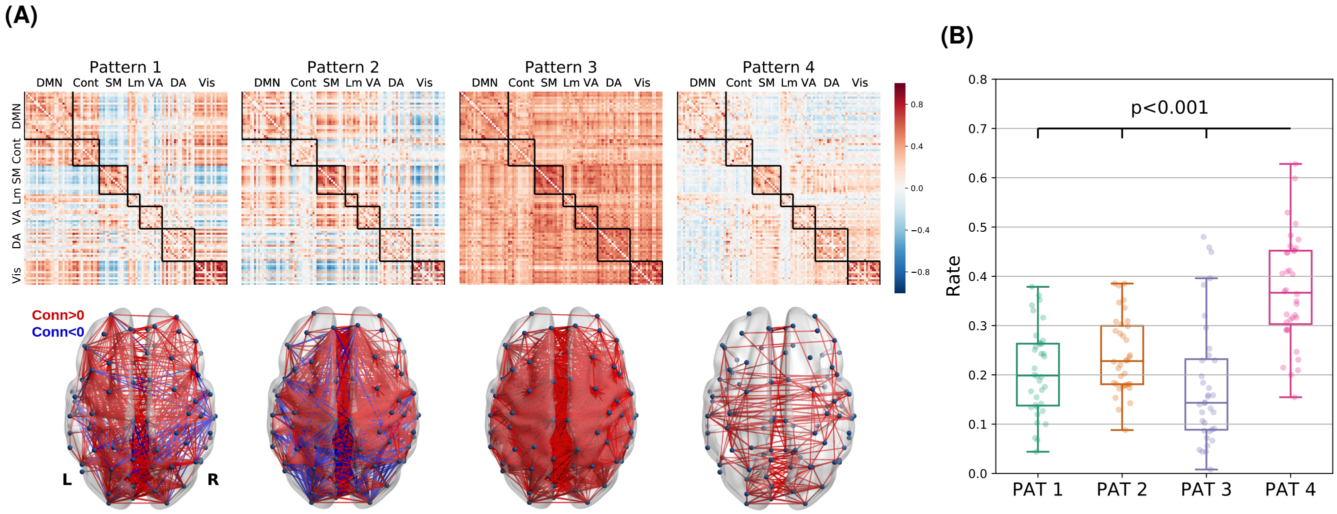

Figure 3. Four distinct signal configurations were recurrently present across resting periods. **(A)** Pattern 1 showed complex inter-areal functional configurations, characterized by short- and long-range connectivity, of positive and negative valence. Pattern 2 showed mainly functional anti-correlations between visual areas and regions of other networks. Pattern 3 showed all-to-all positive functional connectivity among the areas of the studied networks. Pattern 4 showed overall low inter-areal connectivity. **(B)** When estimating each pattern's occurrence rate, Pattern 4 had significantly the highest probability to appear across the resting periods while Pattern 3 had the lowest (paired t-tests, FDR corrected at $\alpha = 0.05$). Brain regions are organized in networks as indicated by the Schaefer atlas; 100 regions (DMN: Default Mode Network, Cont: Executive Control Network, SM: Somatomotor, Lm: Limbic, VA: Ventral Attentional, DA: Dorsal Attentional, Vis: Visual). Colorbar indicates coherence values between any pair of regions.

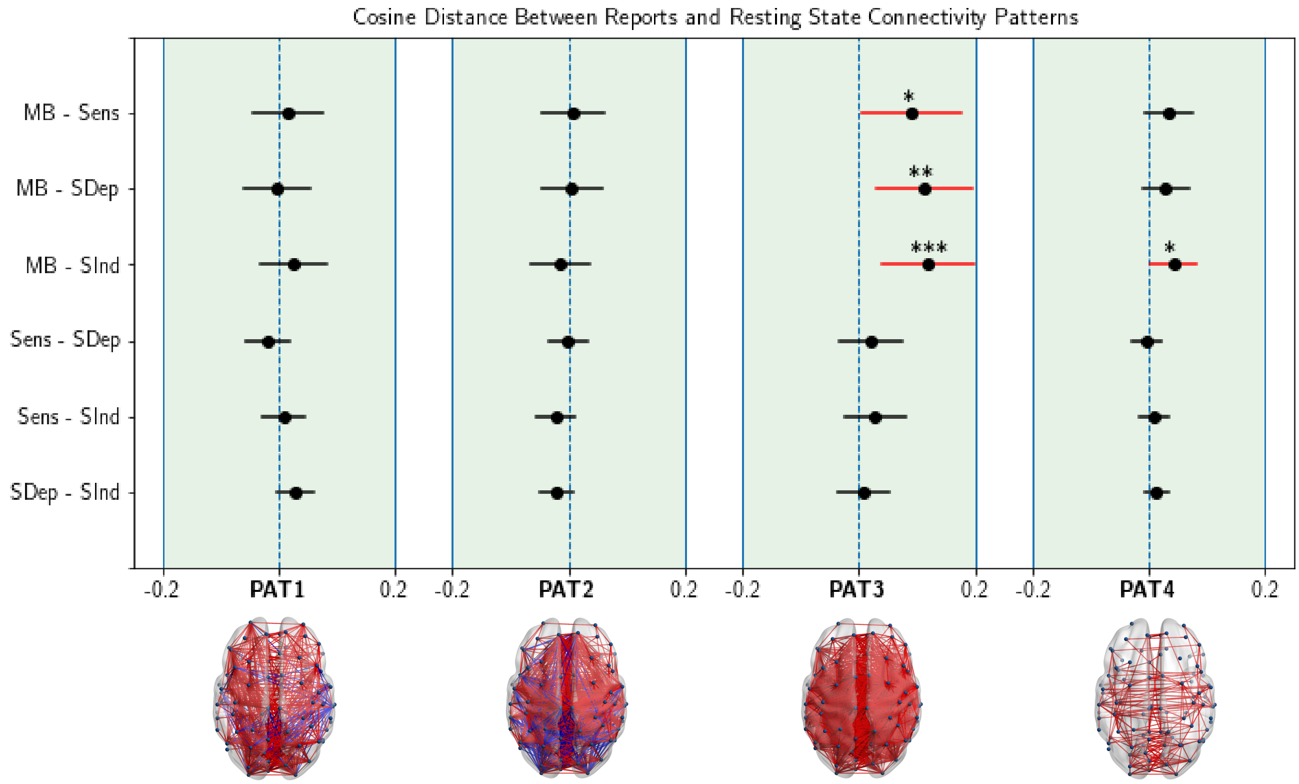

Figure 4. The positive all-to-all inter-areal connectivity pattern was the most similar configuration to MB reports. There was a significant effect of mental state on the distance values to Pattern 3 and Pattern 4. Post-hoc tukey test showed that MB had the highest similarity to Pattern 3 in comparison to all other mind states (error bars indicate asymptomatic confidence intervals around the difference estimate, *p<0.05, **p<0.01, ***p<0.001).

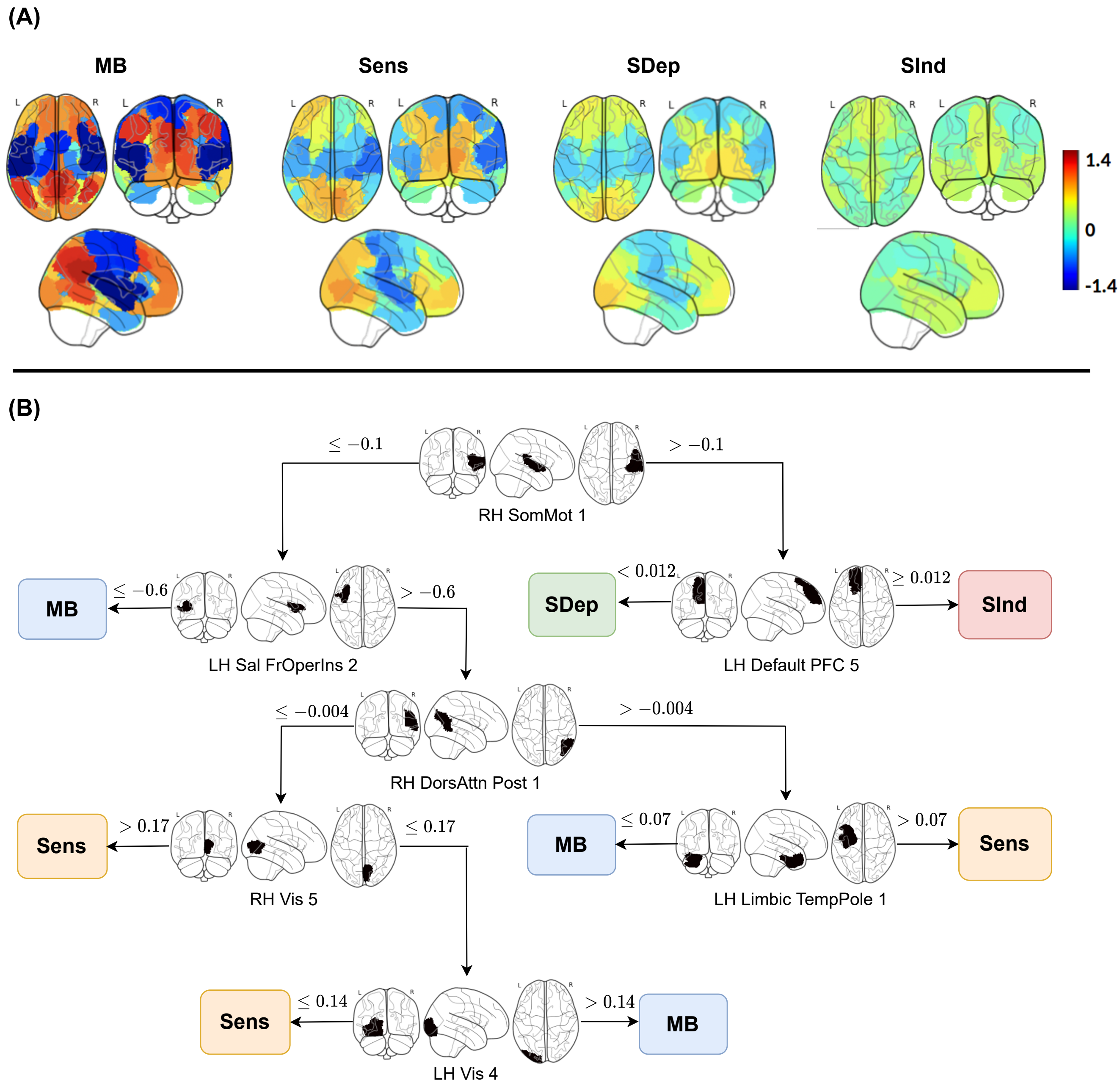

Figure 5. Mind blanking is supported by a segregative brain profile, making it easily classifiable. **(A)** Diffusion map analysis showed a large range in diffusion values for the periods preceding MB reports, leading to two main clusters broadly encompassing the salience network (blue-range cluster), and the DMN (red-range cluster). The identified small area-to-area transition probabilities indicate a less efficient information flow in MB in comparison to content-oriented states. Note: maps indicate averaged diffusion values across subjects, colorbar indicates z score. **(B)** Using the diffusion maps as feature vectors in a decision tree classification scheme, showed that the salience network (somatomotor and insular cortices) was able to classify MB by separating it from thought-related reports in fewer steps. Notes: the "less than" relational operator indicates higher resemblance of that cluster to the salience network (blue-range values); the "more than" relational operator indicates higher resemblance of that cluster to the DMN (red-range values).

Table 1. Confusion matrix of mental state classification using averaged diffusion maps for each mental state of each subject as feature vectors and C4.5 classifier

		Classified as			
		MB	**Sens**	**SDep**	**SInd**
Reported	**MB**	21	8	0	2
	Sens	8	25	0	2
	SDep	0	0	32	4
	SInd	1	0	1	34

Table 2. Classifier performance in classification of each mental state. (FP: false positive, ROC: receiver operating characteristic, TP: true positive).

	TP Rate	**FP Rate**	**Precision**	**ROC Area**
MB	0.677	0.084	0.700	0.838
Sens	0.714	0.078	0.758	0.813
SDep	0.889	0.010	0.970	0.947
SInd	0.944	0.078	0.810	0.917